Novosibirsk terahertz free electron laser: instrumentation development and experimental achievements

2010 Meas. Sci. Technol. 21 054017

(http://iopscience.iop.org/0957-0233/21/5/054017)

Meas. Sci. Technol. **21** (2010) 054017 (13pp) doi:10.1088/0957-0233/21/5/054017

Novosibirsk terahertz free electron laser: instrumentation development and experimental achievements

B A Knyazev[1,2], **G N Kulipanov**[1] **and N A Vinokurov**[1]

[1] Budker Institute of Nuclear Physics SB RAS, 11 Lavrentyeva Ave, Novosibirsk 630090, Russia
[2] Novosibirsk State University, 2 Pirogova Str., Novosibirsk 630090, Russia

E-mail: knyazev@inp.nsk.su

Received 6 November 2009, in final form 4 January 2010
Published 23 March 2010
Online at stacks.iop.org/MST/21/054017

Abstract
Nowadays, the Novosibirsk free electron laser (NovoFEL) is the most intense radiation source in the terahertz spectral range. It operates in the continuous mode with a pulse repetition rate of up to 11.2 MHz (5.6 MHz in the standard mode) and an average power of up to 500 W. The radiation wavelength can be precisely tuned from 120 to 240 mm with a relative line width of 0.3–1%, which corresponds to the Fourier transform limit for a micropulse length of 40–100 ps. The laser radiation is plane-polarized and completely spatially coherent. The radiation is transmitted to six user stations through a nitrogen-filled beamline. Characteristics of the NovoFEL radiation differ drastically from those of conventional low-power (and often broadband) terahertz sources, which enables obtaining results impossible with other sources, but necessitates the development of special experimental equipment and techniques. In this paper, we give a review of the instrumentation developed for control and detection of high-power terahertz radiation and for the study of interaction of the radiation with matter. Quasi-optic elements and systems, one-channel detectors, power meters, real-time imagers, spectroscopy devices and other equipment are described. Selected experimental results (continuous optical discharge, material and biology substance ablation, real-time imaging attenuated total reflection spectroscopy, speckle metrology, polarization rotation by an artificial chiral structure, terahertz radioscopy and imaging) are also presented in the paper. In the near future, after commissioning another four electron racetracks and two optical resonators, intense radiation in the range from 5 to 240 μm will be available for user experiments.

Keywords: free electron laser, terahertz radiation, terahertz optics, terahertz spectroscopy, ablation, optical discharge, radioscopy

(Some figures in this article are in colour only in the electronic version)

1. Introduction

The exponentially growing number of publications devoted to the development of terahertz sources and applications of terahertz radiation reflects the expectation of a breakthrough to new technologies involving this frequency band. The interest in the terahertz radiation is due to its following properties: it is a non-ionizing radiation (the photon energy ranges from 0.04 eV to 0.004 eV); the radiation passes through opaque media and weakly dispersive materials relatively well owing to strong suppression of Rayleigh scattering ($1/\lambda^4$); the frequency range of the radiation covers the region of rotational spectra of molecules, vibrations of biologically important collective modes of DNA and proteins and frequencies characteristic of intermolecular interactions; the terahertz radiation corresponds to the energy region of hydrogen bonds and van der Waals forces of intermolecular interactions.

The invention of broadband terahertz generators, which are based on femtosecond lasers, triggered research in terahertz imaging and tomography, spectroscopy, nonlinear

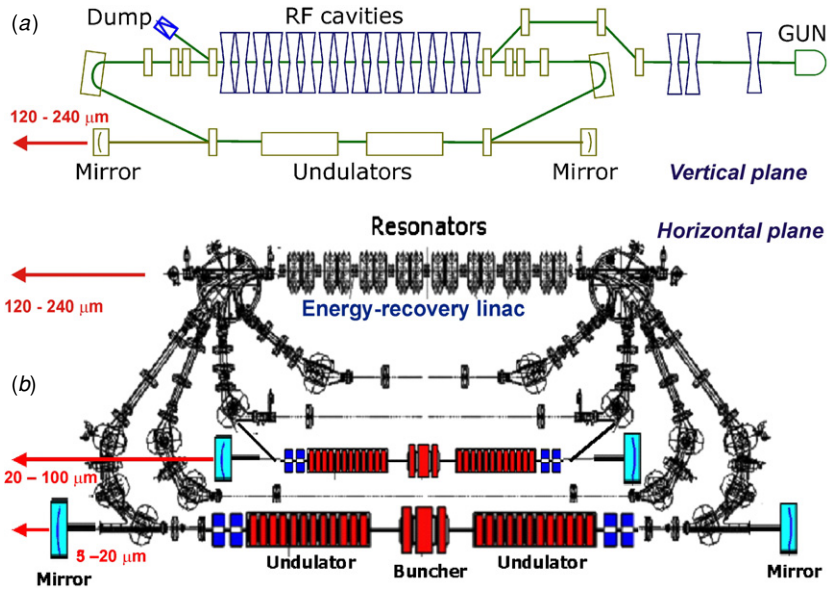

Figure 1. (*a*) Schematic of the terahertz free electron laser; (*b*) the full-scale Novosibirsk free electron laser. The terahertz FEL is in operation, the far-infrared FEL has recently been commissioned, the short-wave FEL is under assembly.

optics, biology and medicine, materials science, security and other applications. In applications which require tunable monochromatic coherent radiation, backward wave oscillators (in the millimeter and high submillimeter regions), injection-seeding parametric generators and difference-frequency generators are commonly used. However, the average power of all the above-mentioned generators is very low. The above-mentioned techniques and methods are described in a comprehensive review [1].

More intense terahertz radiation can be emitted using sources based on the radiation of relativistic electrons in magnetic structures such as synchrotrons and free electron lasers (FEL) [2]. The average radiation power of conventional terahertz free electron lasers at the laboratories of Stanford [3], UCSB [4], FOM-Institute [5], Osaka [6], INEA [7] and KAERI [8] is close to 1 W. Because of the relatively low FEL efficiency, any further increase in the output power can only be achieved using energy-recovery systems. The capabilities of such a technique have been demonstrated on the near-infrared FEL (JFEL), which has recently been commissioned at Jefferson Laboratory [9] and is based on an energy recovery linac (ERL). Now it generates broadband radiation in the near- and mid-infrared spectral ranges with an average power as high as 10 kW. The same facility is also used as a 100 W average-power radiation source, which emits broadband terahertz radiation when a subpicosecond electron bunch passes bending magnets (coherent synchrotron radiation in the THz region).

In this paper we give a brief description of the ERL-based terahertz Novosibirsk free electron laser (NovoFEL) and the survey of the instrumentation developed for experiments with laser radiation. Examples of experimental results achieved at the facility are also presented.

2. Novosibirsk terahertz free electron laser and user stations

Novosibirsk high-power free electron laser (NovoFEL) [10] differs from other ERL-based FELs [9, 11] in low-frequency (180 MHz) non-superconducting RF cavities and a longer wavelength operation range. The first stage of the Novosibirsk free electron laser, generating terahertz radiation, was commissioned in 2003 [12]. It is (figure 1(*a*)) a FEL based on a single-pass ERL with the following parameters: the electron energy is 12 MeV; charge per bunch is 1.5 nC; the bunch repetition rate is 5.6, 11.2 or 22.5 MHz; the maximum average current is 30 mA and the bunch duration is 40–100 ps. Two identical 4 m electromagnetic planar undulators, having a period of 120 mm, a gap of 80 mm and an undulator parameter K of up to 1.2, are installed in the long straight section of the ERL. The principle of free electron laser operation has been described in many publications (e.g. in [13]).

The laser resonator [14] consists of two water-cooled spherical mirrors made of gold-plated copper. Their curvature radius is 15 m and the distance between the mirrors is 26.6 m. The front and rear mirrors have openings 3.5 mm and 8 mm in diameter, respectively. The calculated transparency of the mirror with the 8 mm hole at a wavelength of 150 μm is 1.5%. At this wavelength, the measured round-trip loss is near 7%. The output radiation passes through two windows, which separate the ultrahigh vacuum system of the resonator and accelerator from the atmosphere. Behind the front mirror, an additional iris and a normal-incidence quartz window are installed. Behind the rear one, there is a diamond window, tilted at the Brewster angle.

The laser generates tunable monochromatic radiation within the spectral range of 110–240 μm at the first harmonic, 60–117 μm and 40–80 μm at the second and third harmonics, respectively. The maximum average power for the first harmonic reaches 0.5 kW at a repetition rate of 11.2 MHz

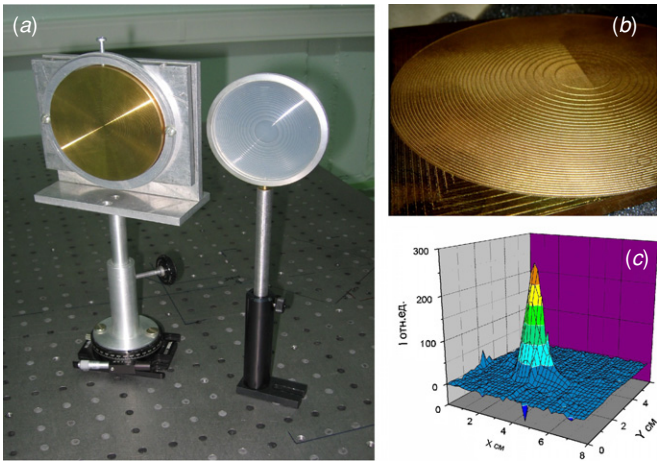

Figure 2. (*a*) Brass Fresnel mirror and high-density polypropylene Fresnel lens; (*b*) mirror profile; (*c*) distribution of terahertz radiation in the mirror focal spot.

(routinely, the laser operates at a repetition rate of 5.6 MHz). The maximum average power of the second and third harmonics is 1.5% and 0.6% with respect to the first harmonic [15]. The micropulse length is about 100 ps, which provides a maximum peak power of about 1 MW. The relative spectral width is 0.25–1%, which is close to the Fourier transform limit. The radiation is completely spatially coherent, and the degree of linear polarization of radiation is better than 99.6% [16].

The radiation of the terahertz FEL, emitted through the mirror opening as a continuous train of pulses, is transmitted through an optical beamline (nitrogen-filled, 16 cm in inner diameter) to the experimental halls. The ultrahigh vacuum system of the FEL and the gas-filled beamline are separated by a diamond window 0.7 mm thick. Six user stations—the metrology station, the photochemistry station, the biological station, the molecular spectroscopy station, the station for radioscopy and spectroscopy and the aerodynamics station—are now in operation (see figure 2 in [17]). The high average power (100–200 W) and large diameter (50–80 mm) of the terahertz beam at the user stations necessitate the development of adequate experimental equipment for radiation control and detection, which is described below.

The full-scale Novosibirsk free electron laser facility is based on the four-orbit 40 MeV electron energy recovery linac. A schematic of the full-scale machine is shown in figure 1(*b*). It is to generate radiation in the range from 5 μm to 0.24 mm [18]. The orbit of the first stage with the terahertz FEL (see above) lies in the vertical plane. The four new turns are being mounted in the horizontal plane. The bypass with the far-infrared FEL has already been assembled in the second straight line section (about 20 MeV energy, figure 1(*b*)). The bypass also provides about 0.7 m lengthening of the second orbit. Therefore, when the bypass magnets are switched on, deceleration of the beam takes place at its third pass through the accelerating system. After that, the electrons come to the first orbit and, after the second deceleration, to the beam dump.

The second-orbit fixed-gap electromagnetic undulator is very similar to the undulators of the first-orbit FEL, but its gap is narrower. The optical resonator length is 20 m (12 wavelengths of the RF system). Therefore, the bunch repetition rate for the initial operation is 7.5 MHz (the 24th subharmonic of the RF system). The water-cooled mirrors are made of copper and covered with gold. Outcoupling holes (3 and 4 mm in diameter) also serve for alignment with a visible reference laser. The first lasing of the FEL in the bypass was achieved in the spring of 2009. At present, it spans the wavelength range from 40 to 80 μm. Optimization of the second laser system as well as the assembly of the third and fourth tracks is in progress.

The architecture and main capabilities of the control and diagnostic system for the Novosibirsk FEL are described in [19]. The software developed for this system employs a client–server model. The software is able to work in both client and server modes. It can also control various pieces of equipment: from the optical cavity mirrors of the FEL to the local equipment of user stations. The mode of control program operation and controlled equipment are determined by external configuration files.

3. Instrumentation for THz beam control and transformation

Since the terahertz (submillimeter) spectral range lies between the regions of 'photonics' and 'electronics', both quasi-optic and electronic techniques have been employed for control, transformation and detection of radiation. Experiments on diffraction using two-slit and bi-mirror Fresnel schemes showed that NovoFEL radiation is completely spatially coherent, whereas the temporal coherence is limited by the radiation pulse length. Polarization characteristics of the laser beam have been examined using a photolithographic polarizer [16]. It was shown that the radiation is practically completely plane-polarized with a polarization degree not less than 99.6%. The last feature enabled using a different combination of photolithographic (from QMC Instruments Ltd and Tydex) and wire-mesh (from Lebedev Physical Institute) polarizers for the control of both polarization direction and intensity attenuation. The polarizers operated properly at a power density of up to 10 J cm^{-2}.

Many materials are sufficiently transparent to the terahertz radiation, but the absorption coefficient of most of them is, however, substantially higher than that of optical materials in the visible spectral range. In a number of experiments (see sections 5 and 6), we focused and imaged terahertz radiation with TPX lenses, whose transparency in both the terahertz and visible regions enabled easy alignment of optical systems. Employment of classical lenses in systems for which a high numerical aperture is critically important (see sections 6.1–6.2) is, however, limited by strong absorption (and, consequently, heating) at the center of a short-focus lens, which may lead to lens deformation and destruction. Using reflective mirrors or diffractive optical elements (DOE) is a solution. A Fresnel mirror, for example, can be cooled easily in comparison with a parabolic mirror. An additional advantage of diffractive elements is the possibility of development of 'focusators'—diffractive optical elements intended for energy

concentration into volumes of certain shapes. Such necessity can arise, for example, in gas-dynamic experiments [20].

Two kinds of diffractive optical elements (figure 2) have been developed and tested using FEL radiation. Circular and elliptical brass mirrors with a parabolic profile of Fresnel zones [21, 22] were fabricated for $\lambda = 130$ μm using a numerical control machine (NCM). The machinery-turned circular Fresnel mirror exhibited perfect focusing with a diffraction efficiency of about 100%, whereas the diffraction efficiency of a simple reflective Fresnel zone plate, produced by etching of a copper clad fiberglass board, was less than 10%. The elliptical Fresnel mirror was drilled with another NCM. Though the surface roughness was 6–10 μm, the diffraction efficiency of the mirror was also close to 100%. A certain Fresnel mirror has to be designed for a given wavelength. A change in the wavelength leads to a change in the focal length and deterioration of focusing. The focal length of high-density polyethylene Fresnel lenses [23] is also proportional to the wavelength, but focusing remains perfect for any wavelength. A radiation resistance test for a Fresnel lens (1 mm thick, 100 mm in diameter) has shown that it works properly in a 100 W terahertz beam.

The large wavelength of terahertz radiation allows using polypropylene (PP) or Mylar (PTE) foils of a thickness much less than the wavelength as effective beamsplitters for high-power beams [24]. High-density PP and PTE foils as well as high-resistance silicon plates are routinely used as windows or path length compensators. The implementation of the quasi-optical elements is described below.

4. THz beam detection and imaging

In the section that follows we will be describing detection methods that encompass the detection of both prompt and thermally induced radiation. Nowadays, highly sensitive photoconductive antennas and electro-optic crystals, which enable coherent detection of the wave electric field, or incoherent far-infrared interferometric systems using cryogenic bolometers, are commonly used for detection of low-intensity terahertz-waves [25]. Such systems are too sensitive to be used for detection of NovoFEL radiation. Single-channel pyroelectric (PE) detectors, linear PE arrays with choppers and, if necessary, a phase lock-in amplifier and different kinds of uncooled bolometers are used for the measurement of radiation intensity. The response time of pyroelectric detectors is not less than 10 ms, whereas that of most bolometers is close to 1 s. Since most of these systems have been developed and calibrated for employment in the visible or infrared regions, they cannot be applied for the measurement of the absolute value of terahertz radiation power. Moreover, the effect of multiple-beam interference in the input windows (and in the semitransparent sensitive elements of some kind of bolometers) dramatically increases in the terahertz region, which leads to considerable variations in the detector sensitivity versus wavelength, incident angle, window wedging, radiation divergence, etc [24]. A technique for absolute power measurement will be described at the end of this section. Fast Schottky-diode detectors [26] were used for recording the NovoFEL micropulse shape with a temporal resolution of 20–30 ps.

The high average power of the NovoFEL enables the development of imaging techniques different from those commonly used (e.g. [1]). Several techniques (figure 3), a near-infrared (NIR) thermal recorder [27], a microbolometer focal plane array (FPA) [28], thermal-sensitive phosphor image plates [29] as well as a thermal-sensitive visible light interferometer [30], have been applied to terahertz beam imaging. Since the photon energy of terahertz radiation is too small to ionize or excite atomic or molecular transitions directly, all these techniques are based on the thermal effect of terahertz radiation. Here we will discuss the advantages and drawbacks of these methods.

The thermal effect is routinely used for detection of radiation in very different spectral regions. The main advantages of this method are its universality and simplicity. The implementation of this technique, however, is a matter of some difficulty. All imagers can be divided into direct detectors, sensitive to terahertz radiation, such as the microbolometer FPA and indirect detectors, which require using an intermediate 'thermal screen'. Another classification attribute is operation in the cw or transient time mode. In cw-mode techniques, temperature distribution gets to a steady state after a short transient time.

In the case of a thermal-sensitive phosphor image plate or a thermal image plate (TIP), terahertz power density distribution can be retrieved via quenching the phosphor screen luminescence induced by UV radiation of a mercury lamp. We used a set of eight $3'' \times 3''$ phosphor screens developed by Macken Instruments Inc. [31] for imaging near- and mid-infrared radiation. Each screen consists of a thin film with a phosphor layer attached to a massive aluminum plate. The screens appeared to be rather transparent to terahertz radiation, and only the two most sensitive screens gave a reasonable response on being exposed to an unfocused laser beam. The magnitude of luminescence quenching versus radiation intensity at a wavelength of 130 μm for the most sensitive thermal image plate #8, model 22-B, is given in figure 4(*a*). Phosphor luminescence was recorded with a 720×576 pixel SONY DCR-TRV230E camcorder. The spatial resolution of the thermal image plate is a convolution of phosphor screen spatial resolution (PSSR), which is limited by transverse thermal conductivity and modulation transfer function of the recorder. The PSSR values for screens #8 and #7 are 1.6 and 0.35 mm, respectively. Apparently, spatial resolution for less sensitive screens is close to the wavelength limit. Thus, a great advantage of thermal image plates is their capability of large-field imaging, but their sensitivity is far from being perfect.

Another imager requiring a thermal screen is the liquid nitrogen-cooled NIR thermal recorder. In our first experiments we used white or black paper as screens, but later, using thermal image plates #5–#7, we obtained a better time resolution. A small array size (128×128 elements) limits the applicability of the thermal recorder in terahertz imaging, but a high repetition rate (up to 50 Hz) enables employment of the device in laser beam tracing.

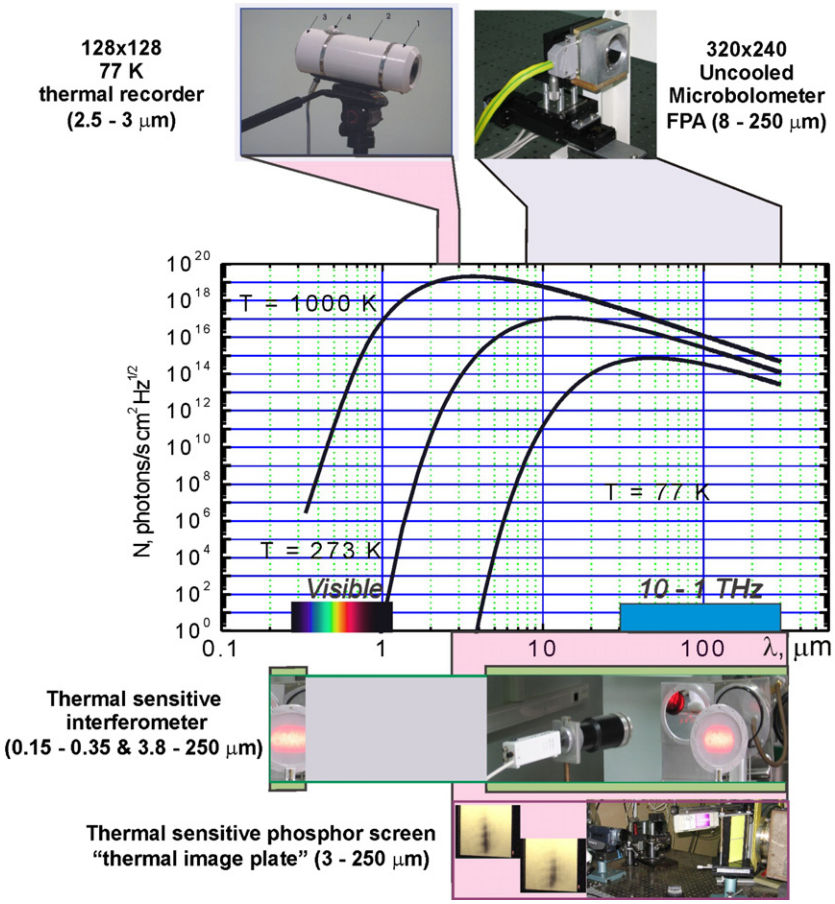

Figure 3. Imaging techniques used for the visualization of intense terahertz radiation.

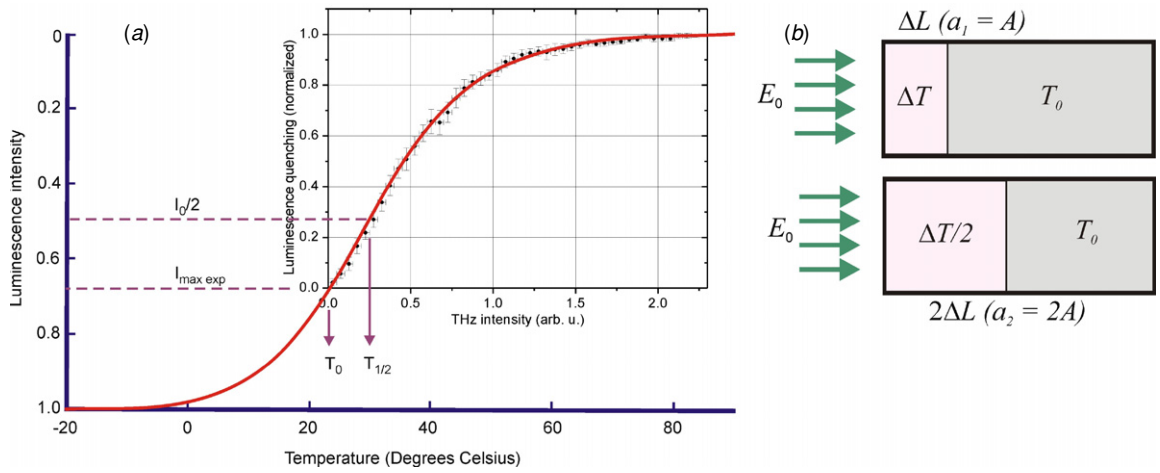

Figure 4. (*a*) Response of the temperature-sensitive phosphor screen (Macken Instruments Inc., thermal image plate #8) to the intensity of incoming terahertz radiation: the red curve is a least-squares four-parameter fitting by the Mott–Seitz law for thermal quenching of luminescence; (*b*) schematics of superficial heat with laser radiation of materials of different thermal diffusivities.

An uncooled 160 × 120 vanadium oxide microbolometer focal plane array (FPA) with a germanium window and physical dimensions of 8.2 × 6.1 mm^2, initially developed by Rzhanov Institute of Semiconductor Physics for detection of mid-IR radiation [32], was adapted to imaging of terahertz radiation [28]. Since the FPA is sensitive directly to terahertz radiation, it turned out to be one of the best terahertz imagers. For $\lambda = 130$ μm, the effective FPA responsivity was $S = 1.6 \times 10^4$ V W^{-1}, the sensitivity threshold was 1.3×10^{-3} W cm^{-2}, the optical noise equivalent power was NEP$_O$ = 200 pW Hz$^{-1/2}$ and the signal-to-noise ratio was SNR = 4×10^3, i.e. more than 70 dB. Real-time imaging was demonstrated at a frequency as high as 90 frames s^{-1}. A novel 320 × 240 pixel matrix with a silicon window more transparent to terahertz

radiation has recently been fabricated by Rzhanov ISP and applied to terahertz spectroscopy experiments (see sections 5 and 6).

The above imagers measure in essence the temperature of an object. Because of a complex dependence of the sensitive element temperature on the incident terahertz radiation intensity, these imagers can perform only relative measurements. To be able to carry out absolute measurements, they have to be calibrated with absolute radiometers. In contrast to these imagers, the thermal-sensitive interferometer is an absolute radiometer. When the shutter gets opened, the radiation under study impinges on a plane-parallel plate transparent to visible light but absorbing the incoming radiation (figure 4(*b*)). If the power density of the incoming radiation is less than the melting and ablation thresholds, and the absorption length is small in comparison with the thermal depth, the target surface temperature increases proportionally to the radiation energy deposited into the target (the reflected radiation is easy to measure). The surface temperature T depends on the thermal diffusivity of the plate material, and, as said above, only a relative power distribution can be retrieved. However, using a coherent laser beam of visible radiation as a probe, and observing an interference pattern produced by two beams reflected from the front and rear plate surfaces, one can determine the absolute radiation power density.

Unlike the surface-temperature-sensitive technique, such a technique probes the energy deposited into the plate volume via a local change in the refractive index and thermal expansion. The areal energy density deposited onto the plate in a moment t after the shutter opening can be calculated easily from the expression [30]

$$E(x, y; t) = \frac{\lambda_0 \rho c_P}{2(\beta + \alpha n)} \cdot \Delta N(t),$$

where λ_0 is the wavelength of the probe beam, ρ and c_P are the material density and thermal capacity, α and n are the linear expansion factor and refractive index, $\beta = \partial n/\partial T$ and, finally, $\Delta N(t)$ measured in 2π units is the phase incursion at a point (x, y) by the moment. Since all the values in the fraction are material and probe radiation constants, the measurement of a number of interference fringes (a real number) gives us an absolute value of the absorbed incident radiation energy. The shorter the measurement time, the smaller the heated layer thickness and the higher spatial resolution. The thermal-sensitive interferometer can operate effectively only for a few seconds, and then it has to be cooled down for the next cycle. Nevertheless, as an absolute power–density meter, it has substantial advantages over classical calorimeters because the measurements are very fast and data processing is very straightforward. The total power of the terahertz beam can be calculated easily via the integration of the power density distribution over the area. Alternative calorimetric techniques used at the facility are described in [33].

5. Instrumentation for THz spectroscopy using monochromatic tunable laser radiation

Most of the existing free electron lasers generate radiation as a short envelope of picosecond pulses. In accordance with the uncertainty relation, the lasing spectrum of such FELs is very wide. When this radiation is used for spectroscopy, the inverse Fourier transform has to be used to retrieve sample spectral characteristics. In contrast, the NovoFEL radiation spectrum is rather narrow, $\delta\lambda/\lambda = (0.3-1)\%$, and the radiation can be treated as quasi-monochromatic. Such a feature is favorable for spectroscopy using no spectral device. Moreover, wide-field spectral-selective radioscopy of substances and objects is possible due to the large cross-section of the laser beam. As an example, we can mention detection of different amino acids buried into Teflon pellets with radioscopy at two laser wavelengths [34].

One of the problems of absorption spectroscopy is the high absorbance of many materials in the terahertz range. For example, most biological substances contain water, which absorbs terahertz radiation completely in a 10 μm layer. For highly absorbing substances, attenuated total reflection spectroscopy [35, 36] is a solution. Using the low beam divergence, 3×10^{-3} rad, first, we developed very simple single- and double-channel THz attenuated total reflection (ATR) spectrometers with a silicon prism as the ATR element and without any other optical elements. The internal reflection coefficients for two radiation polarizations $P = \{p \text{ OR } s\}$ and two incident angles versus the imaginary and real parts of the sample refractive index are shown in figure 5. The large reflectance clearly demonstrates a great advantage of ATR spectroscopy in the study of strongly absorbing materials over classic absorption spectroscopy. FEL tunability allows the determination of both the real and imaginary parts of the sample refractive index via solution of Fresnel equations using reflection coefficients obtained in two measurements at different angles and/or polarizations and matching the results to the pre-calculated matrices $R_1(n, \kappa; \lambda_0, \theta_1, P_1)$ and $R_2(n, \kappa; \lambda_0, \theta_2, P_2)$. A more detailed numerical analysis [37] showed that the optimal experimental strategy for the determination of κ and n would be the measurement of reflection for two different incident angles at p-polarization of probe radiation.

Drawing on this experience, we have developed the first imaging terahertz ATR. The existing imaging ATR spectrometers for the visible and near-infrared spectral ranges [38, 39] consist of a Fourier spectrometer with a CCD detector. They have a very limited field of view ($\sim$1 mm^2 or less), and cannot operate in a real-time mode. The tunability of the Novosibirsk FEL in a wide spectral range as well as a very low beam divergence enables the realization of another kind of imaging ATR spectrometer. A general view of the spectrometer is shown in figure 6. The highly directional radiation of the free electron laser enters through a system of two polarizers into the ATR module at p- or s-polarization. Two mirrors controlled by stepper motors direct the radiation into one of the replaceable silicon prisms through its side edge. The beam impinges on the upper prism edge at an angle exceeding the critical angle of total reflection. A sample under study (liquid, powder, film or solid) is attached to this edge. A system of two mirrors transmits the reflected radiation to an optical system, which images the prism–sample interface onto the microbolometer FPA. The field of view of the spectrometer reaches 200 mm^2.

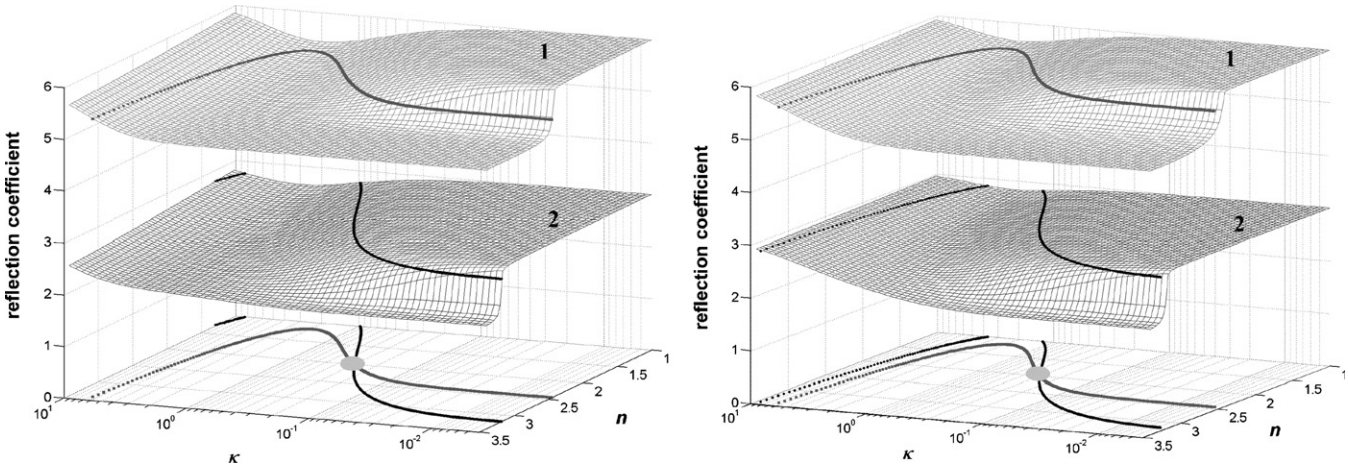

Figure 5. Internal reflection coefficients for the silicon–sample interface versus the real n and imaginary κ parts of the sample refractive index calculated for p (on the left) and s polarizations. The incident angle is equal to 45° for surface 1 and 68° for surface 2. For convenience, the surfaces are shifted up by 2 and 5 units, respectively. The experimentally obtained R_1 and R_2 intersect the calculated surfaces and allow retrieving a unique pair of $\{n, \kappa\}$ (see the gray points) corresponding to the value of the complex refractive index of the sample. In this example, R_1 and R_2 were calculated for water at $f = 2.3$ THz.

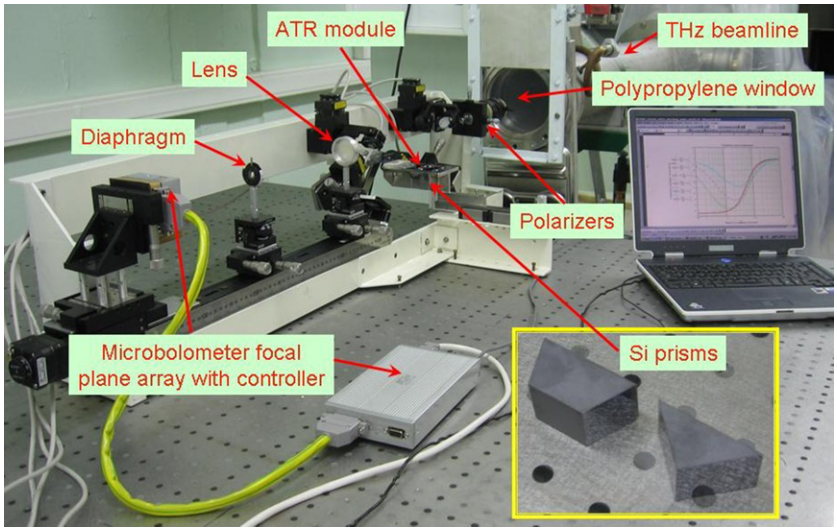

Figure 6. Imaging ATR spectrometer.

The spectrometer can operate in two modes (figure 7). In the first mode, scanning the laser wavelength and using a 320 × 240 microbolometer camera for recording images, one can retrieve the spatial distribution of the spectral characteristics of the sample. In the second mode of operation, the ATR spectrometer can be used to study transient processes at the interface at a fixed laser wavelength. An example of the application of the imaging ATR spectrometer is given in section 6.3.

6. Selected applications

In this section we will cite a number of specific examples which illustrate the unique capabilities for experiments at the user stations of the Novosibirsk free electron laser.

6.1. Interaction of intense laser radiation with gases and solids

High-power lasers are widely used for ignition of optical breakdown in gases in surface processing and production of new materials. They are also routinely used in industry for drilling, cutting and welding. A number of laser types have been used (excimer laser, Nd:YAG laser, Ti:sapphire laser, CO_2 laser, etc) in such applications. Recent experiments on the mid-infrared free electron laser at Jefferson lab [40] have shown that the direct laser synthesis of carbides gives better results in comparison with other lasers. The result of laser–matter interaction depends on both laser wavelength and pulse duration. Experiments in the field of materials science using the NovoFEL, which possesses the longest wavelength among the high-power FELs and a pulse duration intermediate

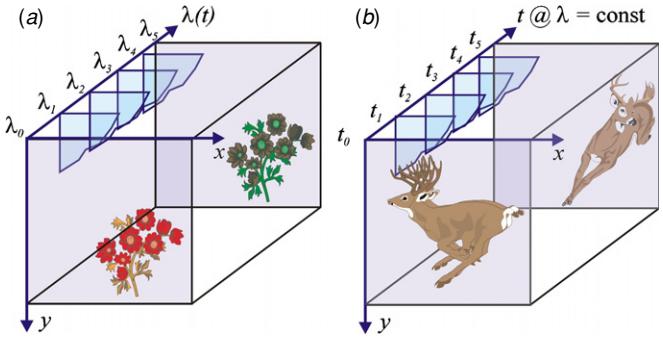

Figure 7. Two operational modes of the imaging ATR spectrometer: (*a*) imaging spectroscopy with continuous tuning of laser wavelength; (*b*) spectrally selective imaging of transient samples at a determined wavelength.

between carbon dioxide and JFEL lasers, apparently seem to be very promising.

By now, two experiments demonstrating the NovoFEL capabilities in materials science have been performed (see figures 9 and 10 in [9]). A simplest example demonstrating the high intensity of the laser is drilling a 5 cm long PMMA block installed directly against the opening ($D = 8$ mm) in the laser resonator mirror using an unfocused laser beam. The block was drilled through within about 3 min due to ablation of the material. Thermal analysis of ablation by NovoFEL radiation in comparison with ablation by a CO_2 laser is given in [41]. The second example is ignition of a continuous optical discharge (COD) in Ar and in air under atmospheric pressure. It was reached by focusing the above-mentioned laser beam with a copper parabolic mirror ($F = 1$ cm). For a numerical aperture of $D/2F = 0.4$, $f = 5.6$ MHz and $P_{\text{average}} \approx 200$ W, the characteristic wave electric field at the focal point was about 1 MV cm^{-1} at a maximum radiation power density of 8×10^8 W cm^{-2}. These values are too small to induce atomic ionization via tunneling or multi-photon processes [42, 43] but rather high for ionization via collisions of seed electrons with gas molecules in an alternative wave field [44, figure 13.20]. It must be emphasized that the terahertz frequency is close to the frequency of electron–atomic collisions under atmospheric pressure; thus, the theory of avalanche ionization in a wave field is here at the limit of its applicability, and a detailed experimental study of terahertz COD would be of physical interest. High pulse repetition rate obviously promotes discharge ignition and sustaining and arouses specific interest in such experiment.

Some of the atmospheric gases, including water vapor, as well as many other molecular gases that can be added to air, have strong absorption lines in the terahertz range. Tuning the NovoFEL wavelength across an absorption line of interest allows controllable deposition of laser energy in a gas. This opens a new opportunity for COD ignition and sustaining as well as for original aerodynamic experiments [20].

6.2. Ablation of biological objects and nanomaterials

Ablation of materials and objects by terahertz radiation is a promising technique for material processing and characterization. Laser radiation from the UV- to mid-IR range is used for the study and identification of high-mass molecules, including biological ones, by the well-known technique of matrix-assisted laser desorption/ionization (MALDI) with a time-of-flight mass-spectrometer [45, 46]. As shown in many papers, the longer the laser wavelength, the softer (non-destructive) is ablation. Since the photon energy of NovoFEL radiation (about 0.01 eV) is ten times less than CO_2 radiation and approximately corresponds to the energies of hydrogen and van der Waals bonds, one can expect to achieve an 'ultra-soft' ablation.

A schematic of terahertz ablation experiments [47] is presented in figure 8(*a*). An aqueous solution with sample molecules was applied on a silicon plate and dried in clean air flow. Then the plate was put into a special glass cell and irradiated with FEL radiation of an average power of 20 W cm^{-2} at $\lambda = 128$ μm. A flow of nitrogen brought the ablated molecules out of the cell into a diffusion aerosol spectrometer, which was able to measure particle diameters in the range from 3 nm to 200 nm [48].

Ablation of two commercially available enzymes, lysozyme and horseradish peroxidase, showed that in each case the aerosol particles produced exhibited only a single distribution mode. The particle size was about 60 nm for lysozyme and 100 nm for horseradish peroxidase, which correlated with their respective molecular weights. The presence of only one fraction enables one to conclude that the ablation of both enzymes was nondestructive and the ablated molecules conserve their primary native structure. The bioanalytical examination of the products revealed retention of their enzymatic activity. In a similar way, the ablation of a mixture of DNA plasmid pUC18 (2.8 tbp) and lambda phage DNA (48 tbp) was carried out. In this case, again, only two peaks corresponding to two different DNAs in an aerosol phase with particle sizes of 7 nm and 70 nm, respectively, were detected. These results clear a way to development of new biotechnologies. The technique was already used to demonstrate a technology for the direct analysis of target DNA at the biochip surface [18].

The same technique can be used to study nanoparticles of different nature: nanopowders, nanopharm drugs, nanotubes and so on. The results of measurements of particle composition in a mixture of fullerene-like complexes based on molybdenum (Mo368) with a general formula $HxMo_{368}O_{1032}(H_2O)_{240}(SO_4)_{48}$, synthesized at the Institute of Inorganic Chemistry SB RAS (V P Fedin), are presented in figure 8(*b*). The complex has a characteristic size of 5.6 nm. Nondestructive ablation has been achieved in the case of this system. The distribution of the aerosol particle size shown in the figure has two maxima, which are likely to correspond to the solitary and adhering complexes. Parallel electron microscopic measurement of the disperse composition of ablation products gave a similar result. Particle size measurement with a diffusion spectrometer was of the same accuracy as that with an electron microscope. Thus, a diffusion spectrometer used in combination with mild terahertz ablation enables high-speed particle size detection. An additional merit of this technique is the simplicity of sample preparation.

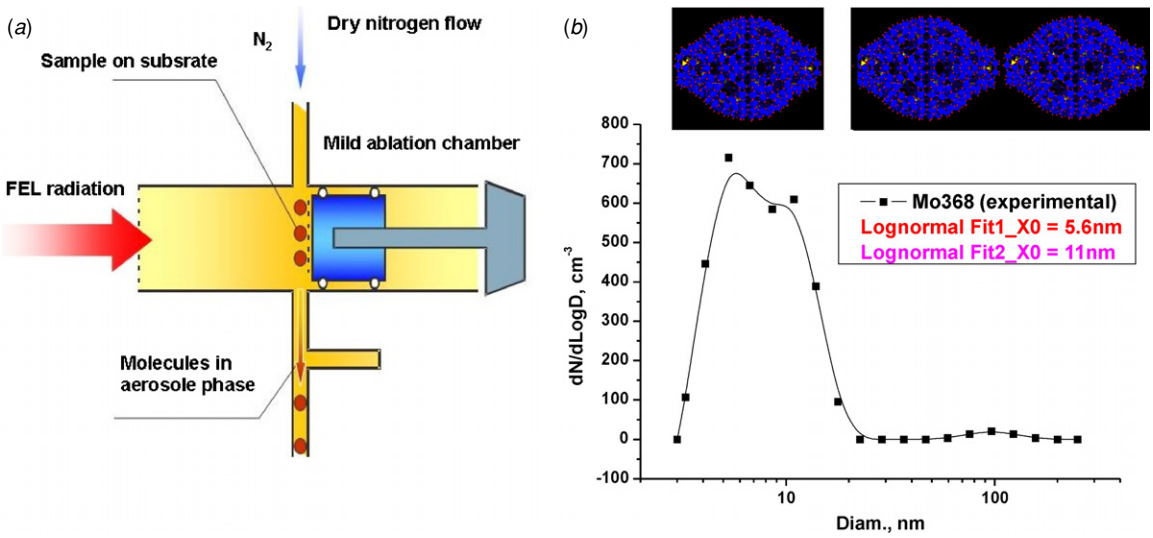

Figure 8. (*a*) Schematic of the experiments on ablation of materials; (*b*) diameters of two fractions detected by the diffusion spectrometer after ablation of fullerene-like molybdenum complexes.

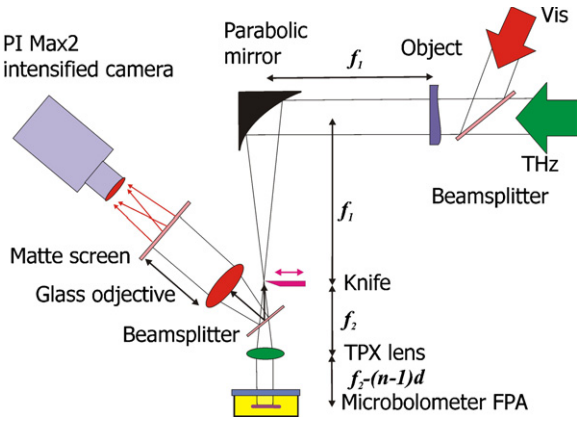

Figure 9. Toepler system to study object non-uniformities with real-time imaging operating in the visible and terahertz spectral ranges. Polypropylene films are used as beamsplitters. The parabolic mirror has a clear aperture of 50 mm and a focal length of 250 mm, TPX lens has a focal length of 100 mm.

6.3. Spectroscopy and spectral selective radioscopy

The tunability of the NovoFEL radiation wavelength and the low beam divergence was employed in many spectroscopy experiments. Terahertz radioscopy ('terascopy' by analogy with 'roentgenoscopy') of objects is the simplest mode of spectroscopy using the NovoFEL. In section 5 we already mentioned the experiment on the detection of L-glutamine and L-cystine amino acids buried in Teflon tablets. Images of different items inside paper and cardboard envelopes, plastics with inner cavities, bones of intact (Wistar) and senescence-accelerated (OXIS) laboratory rats [49] etc were obtained at different wavelengths. All the radioscopic images with the field of view of 50–80 mm were recorded using the imagers described in section 4 at a speed of 20–90 frames s^{-1}.

In a more sophisticated variant, the spectral selective radioscopy system is capable of detecting internal and external non-uniformities of objects. Terahertz radiation has already been applied to pulsed and continuous-wave terahertz imaging and sensing of damage and defects in space shuttle insulating foam and carbon fiber materials [50]. Application of the NovoFEL makes it possible to accelerate the inspection of materials and perform it in real time. One of the spatial-frequency filtering radioscopic systems developed at the NovoFEL facility is shown in figure 9. It is based on a Toepler scheme [51] with a knife-shaped edge as the spatial frequency filter. A particular feature of the system is the possibility of simultaneously operating in both the visible and terahertz spectral regions by using an off-axis parabolic mirror and an achromatic TPX lens transparent in both regions. The application of the microbolometer FPA in combination with a Princeton Instruments ICCD camera enabled real-time imaging. The system was applied to the study of deformation and destruction of plastic films and solids.

The spectroscopic characteristics of metamaterials have also been studied using NovoFEL radiation. The resonant rotation of the polarization plane by a chiral structure fabricated at the Institute of Semiconductor Physics SB RAS has been demonstrated in the range of 1.6–2.3 THz for the very first time [52]. The chiral structure was an array of one-turn helices made of InGaAs/GaAs/Ti/Au film (the unrolled length of the helix is 75 μm and the array density is 500 helices mm^{-2}). Polarization orientations of the incident and transmitted waves were found using a rotating polarizer with a detector (figure 10(*a*)). At a wavelength of 142 μm, the polarization rotation angle α was equal to 17°, whereas at 139 and 158 μm it was 3° and 2°, respectively (see figure 10(*b*)). The observed polarization rotation by the monolayer of helices exceeded the optical rotation for the best liquid crystals of comparable thickness (in the wavelength units) by a factor of a few tens. Materials with negative refractive index in the terahertz range are expected to be created using the helices.

To compare the features of the terahertz imaging ATR (imATR) spectrometer described in section 5 with those of

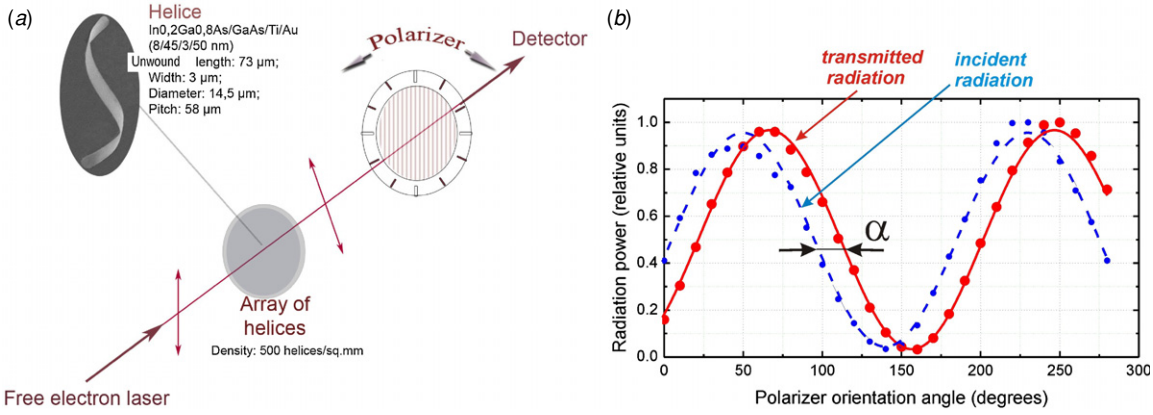

Figure 10. (*a*) Experimental setup for the detection of polarization rotation by an artificial chiral structure; (*b*) intensity of the terahertz wave passing through the polarizer versus polarizer orientation: the dotted curve—without the helix array, the solid curve—transmission through the array at $\lambda = 142$ μm.

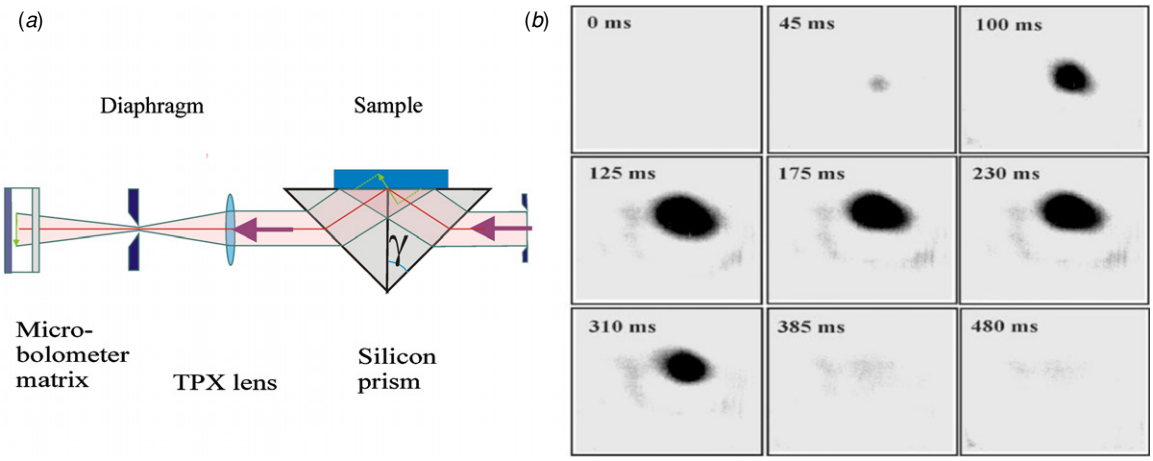

Figure 11. (*a*) Schematic of the experiment with a simplified version of the imaging ATR spectrometer; (*b*) frames selected from the 'terahertz video' recorded with the microbolometer FPA during the injection of an ethanol drop into water, $\lambda = 130$ μm.

well-known systems for the visible and near-infrared regions, we temporarily equipped the spectrometer shown in figure 6 with a glass prism and Princeton Instruments Max2 ICCD camera in place of the silicon prism and microbolometer matrix. A diode-pumped neodymium laser generating radiation at the second harmonic of 0.53 μm was used as the source. Images of many dynamic objects (spreading of a water drop falling on a prism, iodine spot sublimation, intermixing of liquids, etc) as a function of time were recorded at a frequency of tens of frames per second [37]. Excellent temporal and spatial resolution was achieved in this case, even though the optical system imaged not the interface itself but a plane (shown by the green arrow) that was normal to the laser beam optical axis. Such a feature can be explained by an extremely low divergence of the laser beam. The interface image is simply 'projected' onto the image plane.

Images in the terahertz spectral range suffered from strong diffraction. To study the operation of the imATR spectrometer in a terahertz beam in detail, we simplified (figure 11(*a*)) the spectrometer configuration by removing four mirrors of small diameter (20 mm), which appeared to be the main source of diffraction. Figure 11(*b*) demonstrates the real-time images of the terahertz beam reflected from the interface during the injection of ethanol into a water pool (the incidence angle was 57° and the laser wavelength was 130 μm) recorded in this configuration. Since absorption of ethanol is very low in comparison with absorption of water, the reflection coefficient of areas with the silicon–ethanol interface has to be close to unity. The pictures clearly show the ethanol drop dynamics, appearance of 'jets' and some 'trace' at the interface after dissolution of the drop. Nevertheless, the drop boundaries in the images were not absolutely sharp.

There are two causes of dithering of the images. The first cause is a low numerical aperture of the optical system. The second cause is diffraction of the laser beam at the prism–sample interface (in fact, by non-uniformities of the sample refractive index). Both causes have no practical effect in the visible spectral range because of the low beam divergence and short wavelength, but they become of high importance in the terahertz range. It is planned to improve the image quality via increasing the numerical aperture of the optical system and using large aperture mirrors because diffraction at the interface cannot be suppressed in this way. The two methods of image quality improvement are now under examination. The

first method is recording a sequence of interface images via fast moving the imager along the optical axis, which enables spanning the image planes over all parts of the interface, with following computer reconstruction of the whole image. A drawback of this method is a decrease in the time resolution. The second method is splitting the laser beam into an object beam and a reference one and recording a hologram, which enables digital reconstruction of the interface image.

Another spectroscopy technique, which seems to be very promising for the study of thin films and conductor–dielectric interfaces using the NovoFEL as a THz source, is surface plasmon spectroscopy (see, e.g., [53]). Laser beam monochromaticity and tunability enable the implementation of experimental configurations quite different from standard experiments with surface plasmon polariton (SPP), in which the time-domain spectroscopy technique is commonly used (see [54, 55]). Due to the high power of NovoFEL radiation, real-time images of the evanescent wave of terahertz SPP have been obtained using the microbolometer camera. Results of this experiment as well as of experiments on surface plasmon transport along gold films (clear and covered with nanoparticles and DNA) will be published elsewhere.

6.4. Holography, tomography and interferometry

The feasibility of terahertz spectral selective holography and tomography has been demonstrated in a number of experiments [34]. Real-time terahertz imaging of objects illuminated with unidirectional and diffuse terahertz beams has been examined. Speckle patterns, which were observed in the THz region for the very first time, were used for the demonstration of terahertz speckle photography [56, 57]. A laser beam illuminated a diffusely scattering spinning object. The scattered radiation illuminated another object, whose image was recorded with the microbolometer 'video camera'. The speckle pattern, moving across the image plane, enabled the determination of mechanical characteristics of the rotating object. The rotation axis position, instantaneous rotation speed and damping decrement were found from the video, though the object under study was out of the field of view of the recording system. Since a wavelength in the terahertz range is about 200 times longer than a wavelength in the visible range, terahertz speckle metrology (speckle photography and speckle interferometry) must be promising for measurements in the corresponding dimension scale.

Another effect, which can be applied for metrology, is the Talbot effect [58]. The Talbot effect states that any amplitude distribution, which is a periodic function of x and y, will also be periodic in the direction of propagation (z) when z is a multiple of the so-called Talbot distance [59]. This effect is well known in visible light and in quantum mechanics but has not been described in the terahertz range yet. We have recently observed this effect using NovoFEL radiation. The experimental results will be published soon.

By now, terahertz tomography has been demonstrated using wideband picosecond pulses [60]. A very special digital method was used for 2D and 3D image reconstruction. With NovoFEL radiation, classic tomographic schemes can be used in the terahertz range. The crucial difference between visible and terahertz tomography is the very strong diffraction in the second case, which requires development of more complex reconstruction techniques. Simple Gabor holograms have already been recorded at the facility and further experiments are in progress.

7. Concluding remarks

Invention of novel radiation sources was usually followed by implementation of the new spectral range into practice. For example, the period between the discovery of x-rays and their employment in medicine was about 25 years. Development of terahertz sources started about 20 years ago. We can expect real implementation of 'T-rays' in the near future. The results obtained at the NovoFEL user facility have demonstrated a number of techniques based on monochromatic terahertz sources and their possible application. The development of new monochromatic terahertz sources (compact free electron lasers [61], quantum cascade lasers [62], etc) will allow imparting new methods and techniques for employment in medicine, materials science, industry, metrology and many other fields.

Acknowledgments

This work was supported in part by grants from the Russian Foundation for Basic Research (07-02-13547, 09-02-12158 and 09-02-12121) and Siberian Branch of Russian Academy of Science (Integration grant #89). The authors are indebted to the members of the NovoFEL team and NovoFEL users V S Cherkassky, E N Chesnokov, Yu V Chugui, M A Dem'yanenko, D G Esaev, N G Gavrilov, V V Gerasimov, Ya V Getmanov, T N Goryachkovskaya, E I Kolobanov, A S Kozlov, V V Kubarev, S B Malyshkin, A N Matveenko, L E Medvedev, S V Miginsky, L A Mironenko, E V Naumova, V K Ovchar, S E Peltek, A K Petrov, V M Popik, V Ya Prinz, T V Salikova, M A Scheglov, S S Serednyakov, O A Shevchenko, A N Skrinsky, M F Stupak, M G Vlasenko, V I Yakovlev and many others for their significant contribution to the development of the NovoFEL facility and instrumentation as well as for kind permission to cite their results in this paper.

References

[1] Mickan S P and Zhang X-C 2003 T-ray sensing and imaging *Int. J. High Speed Electron. Syst.* **13** 601–76
[2] Carr G L, Martin M C, McKinney W R, Jordan K, Neil G R and Williams G P 2002 High-power terahertz radiation from relativistic electrons *Nature* **420** 153–6
[3] Schwettman H A, Smith T I and Swent R L 1996 Status of the Stanford Picosecond FEL Center *Nucl. Instrum. Methods Phys. Res.* A **375** 662–3
[4] Ramian G and Elias L 1988 The new UCSB compact far-infrared FEL *Nucl. Instrum. Methods Phys. Res.* A **272** 81–8
[5] van der Meer A F G and van der Wiel M J 1997 Mid-IR FEL user facility FELIX *Appl. Spectrosc.* **51** 574–5
[6] Nishimori N, Hajima R, Nagai R and Minehara E J 2001 High extraction efficiency observed at the JAERI free-electron laser *Nucl. Instrum. Methods Phys. Res.* A **475** 266–9

[7] Ciocci F, Bartolini R, Doria A, Gallerano G P, Giovenale E, Kimmitt M F, Messina G and Renieri A 1993 Operation of a compact free-electron laser in the millimeter-wave region with a bunched electron beam *Phys. Rev. Lett.* **70** 928–31

[8] Jeong Y U *et al* 2001 First lasing of the KAERI compact far-infrared free-electron laser driven by a magnetron-based microtron *Nucl. Instrum. Methods Phys. Res.* A **475** 47–50

[9] Neil G R *et al* 2000 Sustained kilowatt lasing in a free-electron laser with same-cell energy recovery *Phys. Rev. Lett.* **84** 662–5

[10] Gavrilov N G *et al* 2007 Status of the Novosibirsk high-power terahertz FEL *Proc. Int. Conf. on Free Electron Lasers (Liverpool, UK)* p 5 Paper TUOD01

[11] Minehara E J 2002 Highly efficient and high-power industrial FELs driven by a compact, stand-alone and zero-boil-off superconducting RF linac *Nucl. Instrum. Methods Phys. Res.* A **483** 8–13

[12] Antokhin E A *et al* 2004 First lasing at the high-power free electron laser at Siberian center for photochemistry research *Nucl. Instrum. Meth. Phys. Res.* A **528** 15–8

[13] Marshall T C 1985 *Free-Electron Lasers* (New York: Macmillan)

[14] Kubarev V V, Persov B Z, Vinokurov N A and Davidov A V 2004 Optical resonator of powerful free-electron laser *Nucl. Instrum. Methods Phys. Res.* A **528** 199–202

[15] Kubarev V V, Kolobanov E I, Kulipanov G N, Matveenko A N, Medvedev L E, Salikova T V, Scheglov M A, Serednyakov S S and Vinokurov N A 2009 Modulation instability at the Novosibirsk Terahertz free electron laser: study and suppression *Proc. 34th Int. Conf. on Infrared, Millimeter and Terahertz Waves (Busan, Korea, 21–25 September 2009)* paper W5E62.0429

[16] Cherkassky V S, Knyazev B A, Kulipanov G N, Matveenko A N, Rudych P D and Vinokurov N A 2007 Study of polarizer characteristics with a high-power terahertz free electron laser *Int. J. Infrared Millim. Waves* **28** 219–22

[17] Knyazev B A, Kulipanov G N and Vinokurov N A 2007 Optical components, detectors and cameras for user-station optical systems at a high-power terahertz FEL *J. Korean Phys. Soc.* **51** 409–15

[18] Kulipanov G N *et al* 2008 Research highlights from the Novosibirsk 400 W average power THz FEL *Terahertz Sci. Technol.* **1** 107–25 http://www.thznetwork.org.cn/Journal/shownews1.asp?id=2

[19] Serednyakov S S, Makashov E V, Palagin K S and Kubarev V V 2007 Control and diagnostic system of Novosibirsk FEL radiation *Proc. 29th Int. Conf. on Free Electron Lasers (Novosibirsk, Russia)* pp 111–3 http://accelconf.web.cern.ch/accelconf/f07/PAPERS/MOPPH043.PDF

[20] Fomin V M, Knyazev B A, Kubarev V V, Kulipanov G N, Scheglov M A, Vinokurov N A, Yakovlev V I and Petrov A K 2007 Research opportunities at terahertz Novosibirsk free electron laser *Proc. Int. Conf. on the Methods of Aerophysical Research (Novosibirsk, Russia, 5–10 February 2007)* (Novosibirsk: Publ. House 'Parallel') pt 2, p 71

[21] Vinokurov N A, Zhigach S A, Knyazev B A, Konysheva A V, Kulipanov G N, Merzhievsky L A, Polskikh I A and Cherkassky V S 2007 Diffractive optical elements and quasioptical schemes on a high-power terahertz free-electron laser *Radiophys. Quantum Electron.* **50** 803–12

[22] Knyazev B A and Cherkassky V S 2006 Reflective diffraction optical elements and their application to control free-electron-laser terahertz radiation *Vestn. Novosibirsk State Univ. Phys.* **1** (2) 3–22 (in Russian) http://www.phys.nsu.ru/vestnik/

[23] Vedernikov V M *et al* 2009 Transmissive diffractive elements for the terahertz spectral range *Proc. 9th Int. Symp. on Measurement Technology and Intelligent Instruments* ed Yu V Chugui vol 2 pp 366–70

[24] Gerasimov V V, Knyazev B A, Rudych P D and Cherkassky V S 2007 Fresnel reflection in optical components and detectors for the terahertz frequency band *Instrum. Exp. Tech.* **50** 524–9

[25] Jiang Z and Zhang X-C 2003 Free-space electro-optic techniques *Sensing with Terahertz Radiation* ed D Mittelman (Berlin: Springer) pp 155–87

[26] Kolobanov E I *et al* 2005 Highly sensitive fast Schottky-diode detectors in experiments on Novosibirsk free electron laser *Proc. Joint 30th Int. Conf. on Infrared and Millimeter Waves and 13th Int. Conf. on Terahertz Electronics (Williamsburg, VA, USA, 19–23 September 2005)* vol 2 (Piscataway, NJ: IEEE) p 154

[27] Kuryshev G L *et al* 1998 Medical infrared imaging system based on a focal plane array for 2.8–3.05 spectral range *Optoelectron. Instrum. Data Process.* no 4 5–10

[28] Dem'yanenko M A, Esaev D G, Knyazev B A, Kulipanov G N and Vinokurov N A 2008 Imaging with a 90 frames s^{-1} microbolometer focal plane array and high-power terahertz free electron laser *Appl. Phys. Lett.* **92** 131116

[29] Knyazev B A and Kubarev V V 2009 Wide-field imaging using a tunable terahertz free electron laser and a thermal image plate *Infrared Phys. Technol.* **52** 14–8

[30] Vinokurov N A, Knyazev B A, Kulipanov G N, Matveenko A N, Popik V M, Cherkassky V S and Shcheglov M A 2007 Visualization of radiation from a high-power terahertz free electron laser with a thermosensitive interferometer *Tech. Phys.* **52** 911–9

[31] http://www.macken.com/thermal.shtml

[32] Dem'yanenko M A, Fomin B I, Ovsyuk V N, Marchishin I V, Parm I O, Vasil'ieva L L and Shashkin V V 2005 Uncooled 160 × 120 microbolometer IR FPA based on sol–gel VO_x *Proc. SPIE* **5957** 59571R.1–59571R.8

[33] Kubarev V V, Makashov E V, Palagin K S, Serednyakov S S and Fedotov M G 2007 Power meters and 2D beam imaging systems on the Novosibirsk Terahertz Free Electron Laser *Conf. Digest of the Joint 32nd Int. Conf. on Infrared and Millimetre Waves, and 15th Int. Conf. on Terahertz Electronics (Cardiff, UK, 3–7 September 2007)* vol 1 ed M J Griffin *et al* (Piscataway, NJ: IEEE) pp 249–50

[34] Cherkassky V S, Gerasimov V V, Ivanov G M, Knyazev B A, Kulipanov G N, Lukyanchikov L A, Merzhievsky L A and Vinokurov N A 2007 Techniques for introscopy of condensed matter in terahertz spectral region *Nucl. Instrum. Methods Phys. Res.* A **575** 63–7

[35] Harrick N J 1967 *Internal Reflection Spectroscopy* (New York: Wiley)

[36] Gerasimov V V and Knyazev B A 2008 Features of attenuated total reflection spectroscopy in the terahertz region *Vestn. Novosibirsk State Univ. Phys.* **3** 97–112 (in Russian) http://www.phys.nsu.ru/vestnik/

[37] Gerasimov V V, Knyazev B A and Cherkassky V S 2010 Spectral-selective real-time images of objects in the mode of attenuated total reflection in visible and terahertz regions *Opt. Spectrosc.* (at press)

[38] Kazarian S G and Van der Weerd J 2008 Simultaneous FTIR spectroscopic imaging and visible photography to monitor tablet dissolution and drug release *Pharm. Res.* **25** 853–60

[39] Burka E M and Curbelo R 2000 Imaging ATR spectrometer *US Patent* No 6.141 100

[40] Schaaf P, Kahle M and Carpene E 2005 Reactive laser synthesis of carbides and nitrides *Appl. Surf. Sci.* **247** 607–15

[41] Zakharov L A, Bulgakova N M, Onischuk A A, Baklanov A M and Petrov A K 2006 Thermal analysis of polymethyl methacrylate ablation by pulsed IR lasers *Proc. SPIE* **6263** 62630S

[42] Popov V S 2004 Tunnel and multiphoton ionization of atoms and ions in a strong laser field (Keldysh theory) *Phys.–Usp.* **47** 855–86
[43] Delone N B and Krainov V P 1985 *Atoms in Strong Light Fields* (Berlin: Springer)
[44] Raiser Yu P 1987 *Gas Discharge Physics* (Moscow: Nauka) (in Russian)
[45] Karas M, Bachmann D, Bahr U and Hillenkamp F 1987 Matrix-assisted ultraviolet laser desorption of non-volatile compounds *Int. J. Mass Spectrom. Ion Process.* **78** 53–68
[46] Tanaka K, Waki H, Ido Y, Akita S, Yoshida Y and Yoshida T 1988 Protein and polymer analyses up to m/z 100 000 by laser ionization time-of-flight mass spectrometry *Rapid Commun. Mass Spectrom.* **2** 151–3
[47] Petrov A K, Kozlov A S, Malyshkin S B, Taraban M B, Popik V M, Scheglov M A, Goriachkovskaya T N and Peltek S E 2007 Nondestructive transfer of complex molecular systems of various origins into aerosol phase by means of submillimeter irradiation of free-electron laser (FEL) of the Siberian center for photochemical research *Nucl. Instrum. Methods Phys. Res.* A **575** 68–71
[48] Julanov Y V, Lushnikov A A and Zagyanov V A 2002 Diffusion aerosol spectrometer *Atmos. Res.* **62** 295–302
[49] Gonchar A M, Gerasimov V V, Gavrilov N G and Knyazev B A 2007 Spectroscopy and spectrally resolved radioscopy of biological substances using terahertz free electron laser radiation *Proc. 29th Int. Conf. on Free Electron Lasers (Novosibirsk, Russia)* pp 86–8 paper MOPPH031 http://accelconf.web.cern.ch/accelconf/f07/PAPERS/MOPPH031.PDF
[50] Redo-Sanchez A, Karpowicz N, Xu J and Zhang X-C 2006 *Proc. 4th Int. Workshop on Ultrasonic and Advanced Methods for Nondestructive Testing and Material Characterization (UMass Dartmouth, N Dartmouth, MA, 19 June 2006)* pp 67–78
[51] Settles G S 2001 *Schlieren and Shadowgraph Techniques: Visualizing Phenomena in Transparent Media* (Berlin: Springer)
[52] Naumova E V, Prinz V Yu, Seleznev V A, Golod S V, Kubarev V V, Knyazev B A, Kulipanov G N, Kuznetsov S A, Kalinin P V and Vinokurov N A 2006 Polarization rotation of THz radiation by an array of helices *Proc. Joint 31st Int. Conf. on Infrared and Millimeter Waves and 14th Int. Conf. on Terahertz Electronics (Shanghai, China, 18–22 September)* p 1 paper WedB4-3
[53] Kawata S 2001 *Near-Field Optics and Surface Plasmon Polaritons (Topics in Applied Physics)* (Berlin: Springer)
[54] Grischkowsky D, Keiding S, van Exter M and Fattinger Ch 1990 Far-infrared time-domain spectroscopy with terahertz beams of dielectrics and semiconductors *J. Opt. Soc. Am.* B **7** 2006–15
[55] Martl M, Darmo J, Unterrainer K and Gornik E 2009 Excitation of terahertz surface plasmon polaritons on etched groove gratings *J. Opt. Soc. Am.* B **26** 554–8
[56] Chashchina O I, Knyazev B A, Kulipanov G N and Vinokurov N A 2009 Real-time speckle metrology using terahertz free electron laser radiation *Nucl. Instrum. Methods Phys. Res.* A **603** 50–1
[57] Vinokurov N A, Dem'yanenko M A, Esaev D G, Knyazev B A, Kulipanov G N, Chashchina O I and Cherkasskii V S 2009 Speckle pattern of the images of objects exposed to monochromatic coherent terahertz radiation *Quantum Electron.* **39** 481–6
[58] Talbot H F 1836 Facts relating to optical science *Phil. Mag.* 401–7
[59] Winthrop J T and Worthington C R 1964 Theory of Fresnel images: I. Plane periodic objects in monochromatic light *J. Opt. Soc. Am.* **55** 373–80
[60] Wang S and Zhang X-C 2004 Pulsed terahertz tomography *J. Phys. D: Appl. Phys.* **37** R1–36
[61] Shevchenko O A, Matveenko A N and Vinokurov N A 2008 Compact ring FEL as a source of high-power infrared radiation *Nucl. Instrum. Methods Phys. Res.* A **603** 42–5
[62] Williams B, Kumar S, Hu Q and Reno J 2005 Operation of terahertz quantum-cascade lasers at 164 K in pulsed mode and at 117 K in continuous-wave mode *Opt. Express* **13** 3331–9